[7]A. Fukuda, Sci. Light **13**, 64 (1964); J. Phys. Soc. Jap. **27**, 96 (1969); Phys. Rev. B **1**, 4161 (1970).
[8]J. F. Marion, Ph.D. thesis (Adelphi University, 1970) (unpublished).
[9]H. A. Jahn and E. Teller, Proc. R. Soc. Lond. A **161**, 220 (1937).
[10]M. C. Stauber, Ph.D. thesis (Adelphi University, 1968) (unpublished).
[11]Allen Nussbaum, Am. J. Phys. **36**, 529 (1968).
[12]The basic B band states are pure triplets ($S=1$) and mix directly only with triplet states. This means that the B band states mix preferentially with the A band states (predominantly triplet) and thus also with the C band states via spin-orbit coupling.
[13]D. Dultz (private communication).
[14]T. Shimada and M. Ishiguro, Phys. Rev. **187**, 1089 (1969).

PHYSICAL REVIEW B VOLUME 7, NUMBER 4 15 FEBRUARY 1973

Chronospectroscopy of Exchange-Coupled Cr^{3+}-Ion Pairs in Ruby*

H. Engstrom and L. F. Mollenauer
Department of Physics, University of California, Berkeley, California 94720
(Received 8 May 1972)

A rather simple method of determining the lifetimes of the excited states of exchange-coupled ion pairs in ruby is described. The technique utilizes a chopped pump light and phase-sensitive detection. It has permitted a great increase in the resolution of optical transitions, and in particular, it allows for a virtual elimination of the vibronic sidebands of the R lines, in order that the true pair spectrum may stand out clearly. Furthermore, transitions originating from different excited levels may be definitely distinguished, thus aiding in the identification of particular transitions with a given pair type. The chronospectroscopic method is of potential value in the studies of energy-transfer mechanisms between single ions and pairs. It has also provided evidence for a fourth-neighbor absorption band at 6050 Å.

I. INTRODUCTION

With the completion of the theoretical work on transition-metal ions by Sugano and Tanabe,[1] the main features of the optical spectrum of ruby ($Al_2O_3:Cr^{3+}$) have been understood. In particular, the two strong sharp-line transitions at 6934 and 6919 Å, the R_1 and R_2 lines, are known to originate in fluorescence on a trigonal-field-split ^2E level and terminate on the ground-state $^4A_2$ level.

In addition to these lines, however, there is a rather large number of transitions beginning at 6852 Å and extending several hundred angstroms toward longer wavelengths for which the crystal field calculations of Sugano and Tanabe were not able to account. Measurements of the intensities of some of these lines as a function of chromium concentration in the Al_2O_3 host lattice indicated that these lines were due to neighboring pairs of Cr^{+3} ions, whose energy levels were shifted from those of the single ions as a result of exchange interactions.[2] Subsequent investigations have confirmed this hypothesis.[3–5]

II. IDENTIFICATION OF PAIR TRANSITIONS

The ground-state interaction of a pair may be described by the Hamiltonian

$$\mathcal{H}=J\vec{S}_1\cdot\vec{S}_2+j(\vec{S}_1\cdot\vec{S}_2)^2\ , \qquad (1)$$

where $|S_1|=|S_2|=\frac{3}{2}$ is the total spin of a single Cr^{3+} ion.[6] This Hamiltonian gives a splitting of the ground state of a pair into four separate levels. Temperature-dependence measurements[4,5,7] of pair transitions yielded values of J and j and tentative assignments of the transitions to specific pairs.

Before the exchange interaction could be fully understood, more positive identification of individual transitions with distinct pair types was required. Initial work was undertaken by Kaplyanskii and Przhevuskii[8] and later and more completely by Mollenauer and Schawlow.[9] In these experiments a static stress was applied in various directions to a sample, thereby lowering the symmetry of the lattice. Transitions of given pair types split in characteristic ways permitting their identification. In this way the N_1 line at 7041 Å was associated with third-neighbor pairs together with the 7058- and 7029-Å lines. The N_2 line at 7009 Å together with lines at 7013 and 7002 Å were shown to be associated with fourth-neighbor pairs.

Nevertheless, many transitions are observable which have not as yet been identified as to pair type.

III. CHRONOSPECTROSCOPIC METHOD

Imbusch once suggested that another way of identifying transitions according to pair type would be to measure the lifetimes of the excited levels.[10] We have been able to do this conveniently using ordinary phase-detection techniques.[11] If the ruby were optically pumped with a light source which is chopped at a frequency ω, the fluorescent transitions would be modulated in intensity at the chopping frequency, and there would be a phase difference between the pump light and the transition which would be determined by the lifetime of the

excited level. This phase difference could be read directly from the lock-in-detector phase-shift control by setting the phase control to null out the signal from the transition. An additional advantage of this method is that the phase control may be set to null out any signal of a given time constant; in particular, the vibronic sidebands of the R lines which appear in the region from about 7000 to 7300 Å, and since they originate on the ^2E level as do the R lines themselves, the vibronics will have an identical time constant. By nulling out the R_1 line, which at helium temperatures is the only strong R transition, one also nulls out the vibronic sidebands.

IV. APPARATUS

Figure 1 shows the experimental apparatus. All but the strong 5461-Å line from a 200-W mercury arc lamp is filtered out using a combination of 5461-Å interference filter and a blue-green-glass Corning filter. This light is then chopped and used to pump a ruby sample approximately 1 mm thick having a concentration of about 0.5-wt% Cr_2O_3 in Al_2O_3. This concentration assured a sufficient number of chromium pairs for strong pair transitions, yet the sample was still thin enough at this concentration to make reabsorption of fluorescent light from the pairs negligible. The pump light was filtered out with a sharp-cut red Corning filter and the fluorescence analyzed with a 1-m Jarrel-Ash grating spectrometer and detected with an EMI 9558Q photomultiplier tube.

Central to the entire apparatus is a Princeton Applied Research model No. HR8 lock-in detector operated in its internal reference mode; that is, the reference oscillator is internal to the lock in. The phase control allows a 360° continuous phase shift and may be read to approximately 1°. This turned out to be not nearly fine enough, so an external fine adjust phase control was added. This control consists merely of a helipot in series with a capacitor. A signal at 50 Hz can be shifted in phase by any amount up to about 10°. From the fine phase adjust the oscillator signal enters a 20-W power amplifier which is used to drive a synchronous motor nominally rated for 30 revolution per second using 60-Hz current. With a two-bladed chopper, pump-light modulation from 30 to 100 Hz could be attained.

If two transitions occur from levels with nearly equal lifetimes, say τ and $\tau+\Delta\tau$, it is not hard to show that the maximum resolution is obtainable when $\omega\tau \simeq 45°$. Since the lifetimes of the R and N lines are known[11] to be from 1 to 10 msec, the

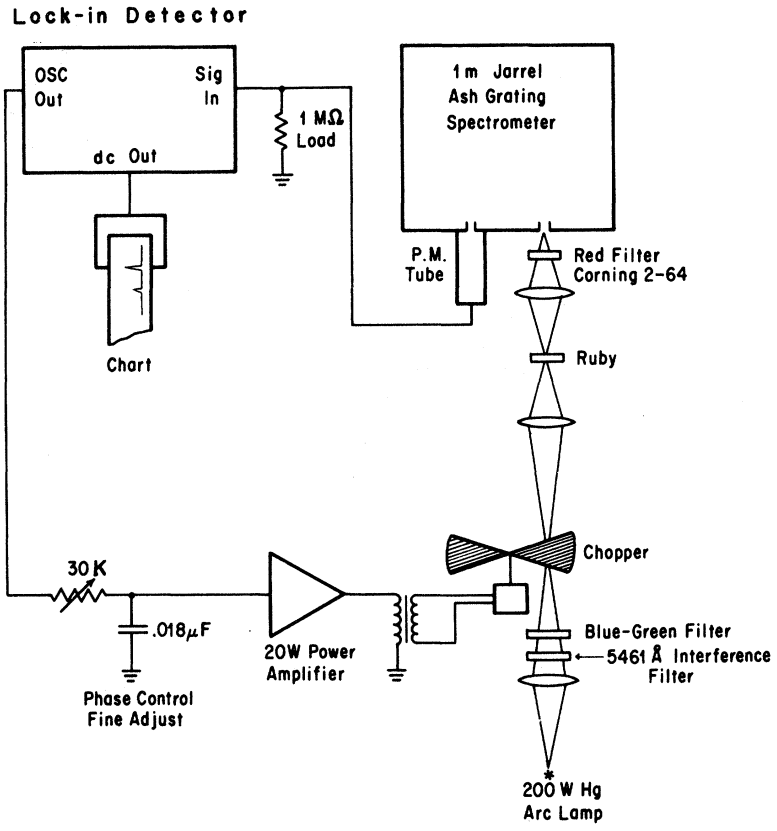

FIG. 1. Block diagram of apparatus for measurements of pair spectrum.

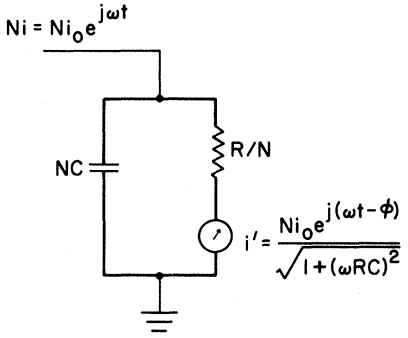

FIG. 2. Equivalent circuit for chronospectroscopic measurements on isolated chromium ions. Ni represents excitation of pair states NC and i' the intensity of the fluorescence.

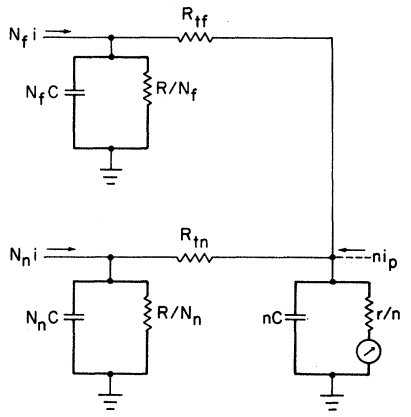

FIG. 3. Equivalent circuit for an ion pair excited by energy transfer from N_n "near" and N_f "far" single ions. R_{tf} and R_{tn} represent energy transfer from far and near single ions to the nC pair states. ni_p represents possible pumping of intrinsic pair bands.

experiments were performed at modulation frequencies of both 45.6 and 72 Hz.

V. ELECTRICAL ANALOG

A simple ac circuit analog is helpful in understanding the experiment. Let us consider for the moment only the isolated Cr^{3+} ions. Each excited state of the ion may be represented by a capacitor of arbitrary value C. A resistor of value R in parallel with C represents the transition to the ground state if the conductance $1/R$ is taken to be proportional to the matrix element of the transition and $R=\tau/C$, where τ is the lifetime of the excited state. If we are pumping N chromium ions there will be N of the excited states for a total capacitance of NC. Similarly there will be N transitions to ground for a total resistance of R/N. Hence our equivalent circuit for any excited state is shown in Fig. 2.

Here $i=i_0e^{j\omega t}$ represents the optical pump intensity of one ion, where ω is again the chopping frequency and the current through the resistor

$$i'=Ni_0e^{j(\omega t-\phi)}/[1+(\omega RC)^2]^{1/2} \qquad (2)$$

represents the total fluorescent intensity of the transition. The phase shift ϕ is trivial to calculate:

$$\tan\phi=\omega RC=\omega\tau\ . \qquad (3)$$

When N becomes sufficiently large so that a significant number of pairs are formed, the picture becomes much more complex due to energy transfer between the single ions and the pairs. Imbusch[12] has done some rather comprehensive experiments on this phenomenon, and his work has been very useful as a guide in our experiments. Imbusch's results could be explained on the assumption that the excited levels of the pairs are populated exclusively through energy transfer from the single ions. Furthermore, in measuring the fluorescence-decay signals from the 7009- and 7041-Å lines, Imbusch noted a double-decay phenomenon consisting of an initial rapid decay (1.1 msec for the case of the 7009-Å line) followed by a slower (10-msec) decay. He attributed this mode of decay to very rapid energy transfer from the single ions near the pair and much slower transfer from those ions more distant.

We may account for such effects in our electrical analog by adding separate RC networks for single ions which are "near" and "far" from the pair; i.e., those ions which transfer energy to the pair essentially instantaneously and those whose transfer times are significantly longer than the intrinsic

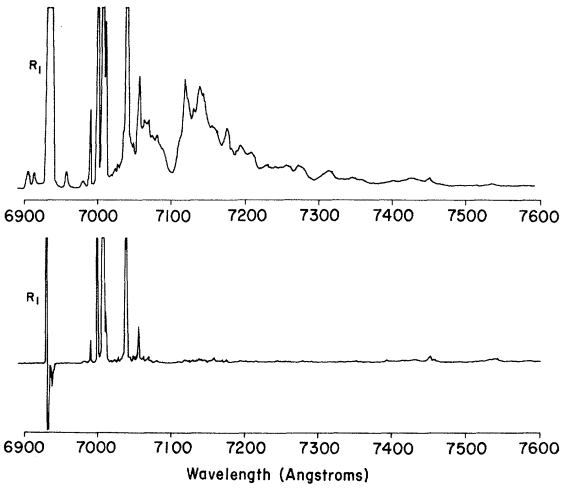

FIG. 4. Ruby pair line and vibronic spectrum at 45.7 Hz and 4.2 °K. Top, lock-in phase set to maximize R_1 line; bottom, phase set to null R_1 line and associated vibronics.

lifetime of the pair. Figure 3 shows the resulting circuit where n is the number of pairs of a given type; N_n is the number of single ions which are near pairs of that type, and R_{tn} represents transfer from those ions to the pairs. The far ions are represented similarly. We expect R_{tn} to be much smaller than R/N_n such that the near ions do not fluoresce in the R_1 line significantly, but transfer their energy to the pairs. The initial decay time will be determined principally by the values of N_n, n, r, and R_{tn}. The dashed line labeled n_{ip} represents a current input corresponding to any intrinsic pumping of pair bands. If we assume that transfer is immediate so that $R_{tn}=0$ and that there is no intrinsic pumping, the initial decay time is simple to calculate in terms of the remaining parameters

$$\tau = rC\left(\frac{N_n}{n}+1\right)\frac{1}{(r/R)(N_n/n)+1} \quad . \tag{4}$$

This circuit is fully analogous to ruby-pair-line fluorescence, and the resulting phase shifts are in qualitative agreement with Imbusch's observations and with ours. Even though the many unknown parameters make exact calculation of phase changes impossible, the fact that the phase difference varies monotonically with r, R_{tn}, and R_{tf} permits us to gain much information from the experiments.

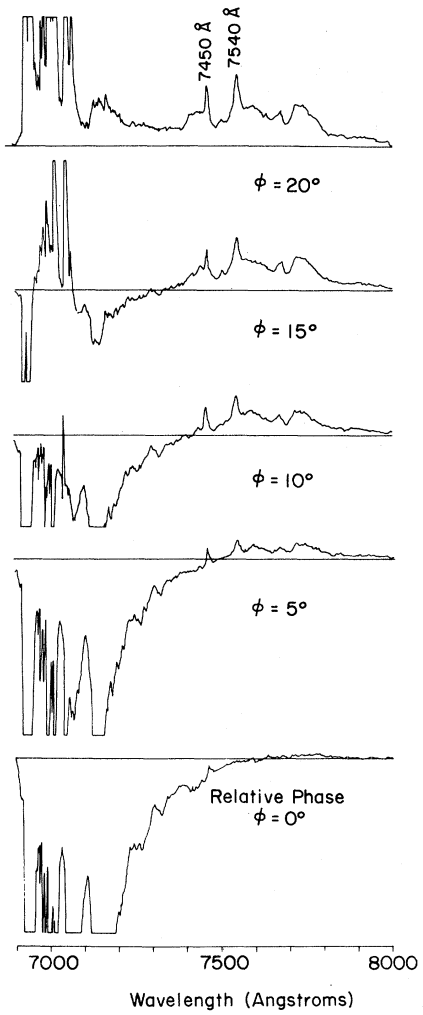

FIG. 5. Ruby-vibronic spectrum at 72 Hz and 77.4 °K indicating that vibronics above 7450 Å are not associated with the R_1 line. Phase angles are given relative to an arbitrary zero.

VI. VIBRONICS AND PAIR SPECTRUM

An important advantage of the chronospectroscopic technique is illustrated in Fig. 4. The top graph shows the ruby spectrum from 6900 to 7600 Å with the phase set to maximize the R_1 line. The broad vibronics of this line are rather strong from 7000 to 7300 Å. The bottom figure shows the same spectrum at the same gain but with the phase set to null out the R_1 line, and its associated vibronic sidebands. Because the lifetimes of the pair levels are much shorter, the pair lines remain rather strong, as is seen.

Not all of the vibronics visible in this region of the ruby spectrum could be eliminated in this manner, however. Figure 5 shows the spectrum for values of lock-in phase incremented in steps of 5°. For the relative phase set to 0° it is seen that the R-line vibronics extend to about 7500 Å. The 7452-Å line already points in a positive direction indicating a very short time constant, while the 7540-Å line is almost completely nulled for $\phi=0°$. For $\phi=5°$ and 10°, there appear at wavelengths longer than 7452-Å vibronics whose time constant is much shorter than that of the R line and its vibronics. The lifetime of these long-wavelength vibronics seems to be close to that of the 7452-Å line itself, and to be shorter than that of any other pair line. For $\phi=15°$ all the pair lines have turned positive and finally the R lines, with the longest lifetimes, have turned over by $\phi=20°$.

The 7452-Å line is known to originate from second-neighbor pairs.[9] If these pairs were very strongly coupled to the lattice, one would expect most of the energy of the excited level to appear in the sidbands with great attenuation of the no-phonon line. Since nonradiative decays are typically very much faster than radiative ones, the assumption that most of the second-neighbor excited-state energy appears associated with vibronic transitions would also account for the very short lifetime of that level.

VII. RESULTS OF INCREASED RESOLUTION

The chronospectroscopic experiments permitted an unexpected increase in the resolving power of our apparatus. They not only enabled us to un-

cover transitions ordinarily obscured by other neighboring transitions, but in many cases yielded some qualitative information as to the structure of the excited-state level. The first of these features is illustrated in Fig. 6 which shows the R_1 line at 4.2 °K as the phase is incremented past the null point. For $\phi = -7.2°$ a small transition near 6932 Å is clearly evident, and this transition has a lifetime significantly shorter than the $\bar{E}(^2E)$ level from which the R_1 line originates. Since short lifetimes tend to be characteristic of pair transitions it is

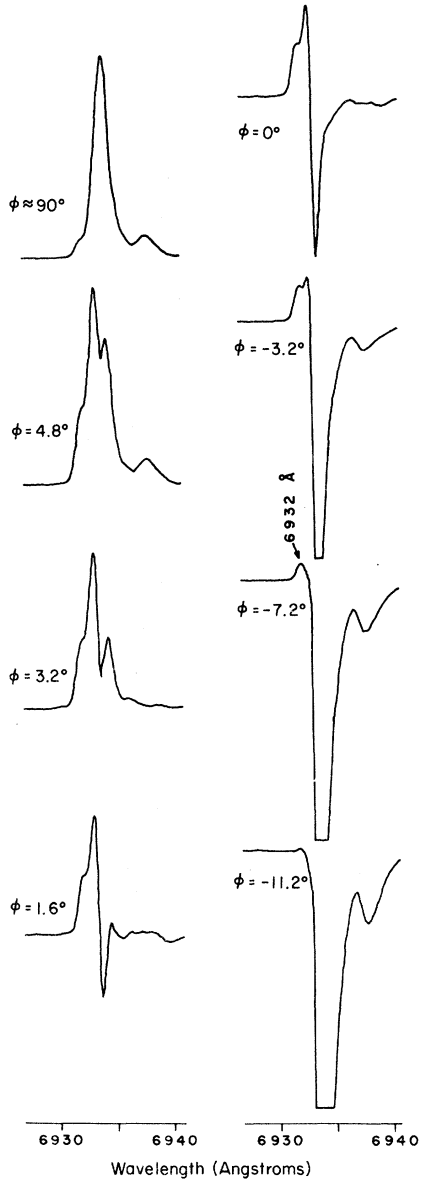

FIG. 6. Null-point crossover of R_1 line permitting resolution of 6932-Å pair line. The diagram for $\phi \approx 90°$ shows the R_1 line at full intensity with 6932-Å line unresolved. Taken at 45.7 Hz and 4.2 °K.

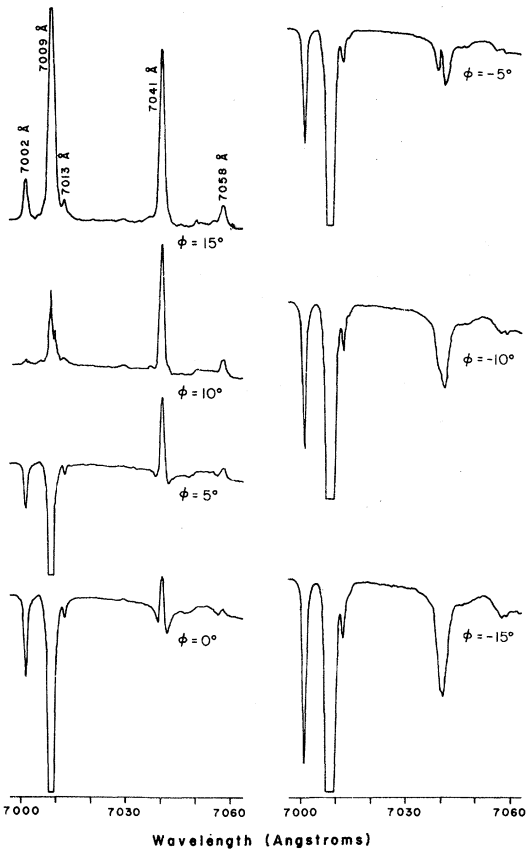

FIG. 7. Null-point crossover of 7009- and 7041-Å lines at 45.6 Hz and 4.2 °K. The center of the 7041-Å line envelope has a shorter time constant than the edges. Phase is given relative to an arbitrary zero.

likely that the 6932 line is a pair line. This transition is likely to be the unresolved doublet consisting of transitions at 6931.51 and 6932.03 Å observed by Jacobs,[13] and which Kisliuk *et al.*[7] believe to originate on pairs more distant than fourth neighbor.

For several of the ruby transitions the line shape at the "null point" either has a dip in the center such as the R_1 line curve for $\phi = 3.2°$, or else it is unsymmetrical in some way. This behavior can arise through any mechanism which changes the time constant of light of a certain wavelength. One such mechanism, which would account for the R_1 line dip, is the phenomenon of self-trapping. That is, light of a wavelength at the center of the transition envelope is more likely to be reabsorbed, thereby lengthening the effective time constant for that wavelength, and thus causing a dip in the center of the envelope.

Not all asymmetry in the curve at the null point is explainable in this way, however, and for some transitions, such as the 7041-Å line, the center of the envelope has a *shorter* time constant than the edges. Such behavior must originate through some

structure in the excited state itself; most likely through the perturbing crystal-strain field which is responsible for the broadening of the lines. Figure 7 shows the null-point crossings of the 7009- and 7041-Å lines.

Figure 8 shows a more detailed set of curves of the null-point crossing of the 7009-Å line. In comparing Figs. 7 and 8 the difference in the rate of crossover as a function of phase is rather striking. At these temperatures in fluorescence the 7009-Å line is about five times as intense as the 7041-Å line. Thus it would be expected that the crossover rate at the null point $dI/d\phi$ would be five times as large for the 7009-Å line as for the 7041-Å line. In fact the crossover rate is about 15 times as great.

Suppose two sinusoidal signals of amplitudes A and B are received at the input of the lock-in detector. If these signals are exactly in phase, the input signal may be expressed as

$$Y=(A+B)\sin\theta\ , \tag{5}$$

where $\theta=\omega t$.

If ϕ is the phase-angle setting of the lock-in, for unity gain the integrated dc output will be simply

$$I=[2(A+B)/\pi]\cos\phi\ . \tag{6}$$

Thus $I=0$ at $\phi=\frac{1}{2}\pi$ and

$$\left.\frac{dI}{d\phi}\right|_{I=0}=\frac{-2(A+B)}{\pi}\ . \tag{7}$$

If, however, the two signals A and B are separated in phase by a small angle α so that the input signal is

$$Y=A\sin\theta+B\sin(\theta-\alpha)\ , \tag{8}$$

one finds that Eq. (6) becomes

$$I=(2A/\pi)\cos\theta+(2B/\pi)\cos(\phi-\alpha) \tag{9}$$

and $I=0$ for $\phi=\frac{1}{2}\pi+\alpha B/(A+B)$. For this value of ϕ,

$$\left.\frac{dI}{d\phi}\right|_{I=0}\simeq-\frac{2}{\pi}\left(A\cos\frac{\alpha B}{A+B}+B\cos\frac{\alpha A}{A+B}\right), \tag{10}$$

which is clearly less, in absolute value, than the value given by Eq. (7).

Thus we may relate the discrepancy between the crossover rates of 7009- and 7041-Å lines to unresolved structure of the excited state of the 7041-Å line. One can think of a level as consisting of an electronic state perturbed by the crystal-strain field, such that the resulting level is broadened. A transition from the upper part of the excited-state envelope to the upper part of the ground state may give the same wavelength photon as a transition between the two centers of the broadened levels, but these two transitions may have different time constants. Suppose at a single wavelength, a continuum of signals with amplitude $A(\alpha)$ and phase $\theta-\alpha$ is detected. Clearly $A(\alpha)$ will be some positive-continuous function of α and will be zero for values of α very different from the null-point phase angle. It is found that the crossover rate will be given approximately by

$$\left.\frac{dI}{d\phi}\right|_{I=0}=-\frac{2}{\pi}\int_{-\alpha_0}^{\alpha_0}A(\alpha)\cos\alpha\,d\alpha\ , \tag{11}$$

where $(-\alpha_0, \alpha_0)$ is the interval over which $A(\alpha)$ is nonzero. This equation is just a simple generalization of Eq. (9). The magnitude of the crossover rate is clearly less than the value

$$-(2/\pi)\int_{-\alpha_0}^{\alpha_0}A(\alpha)\,d\alpha$$

for the case where all signals have the same phase. Thus, we see that transitions between broad levels or levels having much structure may have a sig-

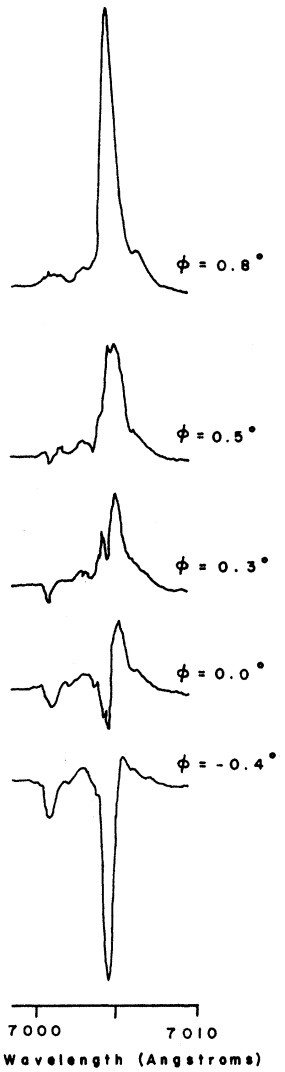

FIG. 8. Null-point crossover of 7009-Å line at 45.6 Hz and 4.2 °K. Phase angle is relative to an arbitrary zero.

nificantly slower crossover rate than sharp-line transitions.

This experiment was repeated with the slits of the spectrometer closed down from 100 to 50 μm. There was no discernible difference in the crossover rate of the 7041-Å line indicating that the result was in fact due to structure in the excited state rather than to the finite dispersion (~8 Å/mm) of the spectrometer.

VIII. RESULTS OF NULL-POINT MEASUREMENTS

Measurements of the amplitudes of the observable pair lines as a function of lock-in phase were plotted for values of ϕ near the null points. Graphs of these amplitudes permitted rather accurate determinations of the null-point phase angles. The results are listed in Table I, where the absolute phase lag of the fluorescent signal with respect to the pump light is given. Column three shows the pair assignment based on the results of the null-point measurements. The results are also displayed in Fig. 9.

Since the pair levels are populated almost exclusively through energy transfer, the rate of energy transfer to each pair type will determine the phase lag of fluorescent radiation, assuming that the decay to the ground state is much faster than the transfer rate. In that case all transitions of a given pair type will have essentially the same null-point phase. As Fig. 9 shows, this assumption seems to be justified in that the null-point phase angles seem to fall into rather well-defined groups. As is seen, the R-line transitions, arising from single ions, both have phases of about 63°. There is a rather large group all lying within a degree or so of 57° and this group includes the 7009-Å line which is known to originate from the fourth-neighbor pair. Thus, it seems reasonable to associate all of these lines with fourth neighbors. Similarly, the group around 54° which includes

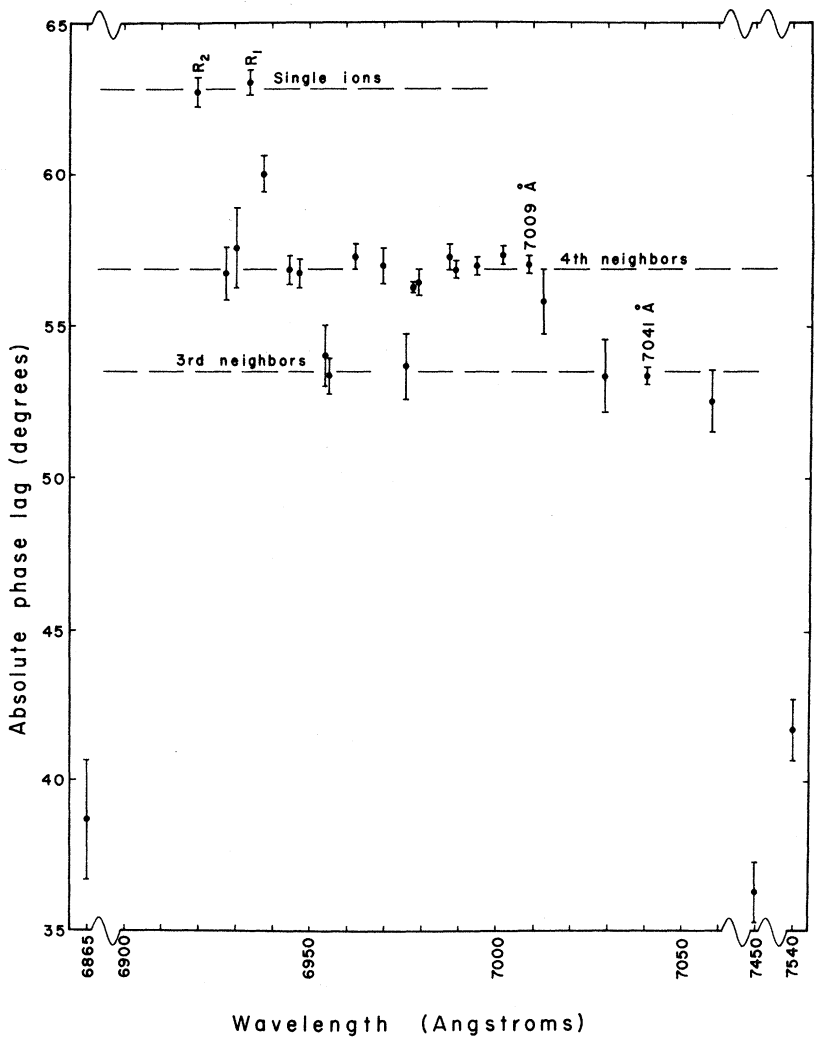

FIG. 9. Null points of ruby-pair lines taken at 72 Hz and 77.4 °K. Horizontal dashed lines indicate assignments for single ions and third- and fourth-neighbor pairs. Phase angles are given relative to the pump-light phase.

TABLE I. Absolute phase lag of the fluorescent signal with respect to the pump light for various pair transitions.

λ (Å)	φ (deg)	Neighbor
6865.6	38.7 ± 2.0	2nd
6919.8	62.7 ± 0.5	*R*
6927.4	56.8 ± 0.9	4th
6930.2	57.6 ± 1.3	4th
6933.8	63.0 ± 0.4	*R*
6937.6	60.0 ± 0.6	more distant than 4th
6944.5	56.9 ± 0.5	4th
6947.1	56.8 ± 0.5	4th
6954.1	54.1 ± 1.0	3rd
6955.2	53.4 ± 0.6	3rd
6962.2	57.3 ± 0.4	4th
6969.6	57.0 ± 0.6	4th
6976.2	54.9 ± 1.1	3rd
6977.8	56.3 ± 0.2	4th
6979.2	56.5 ± 0.4	4th
6987.5	57.3 ± 0.4	4th
6989.4	56.9 ± 0.3	4th
6995.0	57.0 ± 0.3	4th
7001.8	57.4 ± 0.3	4th
7008.8	57.1 ± 0.3	4th
7012.7	55.9 ± 1.1	4th
7029.5	53.4 ± 1.1	3rd
7040.6	53.4 ± 0.3	3rd
7058.2	52.6 ± 1.0	3rd
7452	36.3 ± 1.0	2nd
7540	41.7 ± 1.0	1st

the 7041-Å line may be associated with third neighbors.

Figure 9 also shows the null-point phases of several other transitions. Of these, the 6937.6-Å line, having a null-point phase of 60°, is likely to be due to a more distant neighbor than fourth. Near the bottom of the figure are three more points. The 7540-Å line is thought to come from a first-neighbor pair, and the 7452-Å line from a second-neighbor pair.[9] The 6865.6-Å line is also thought to originate on a second-neighbor pair,[7] but it is so weak in fluorescence that our phase measurements were inconclusive in establishing its pair association. However, our data are certainly not inconsistent with a second-neighbor assignment for this line.

Kisliuk *et al.*[7] have devised an energy-level scheme by fitting the lines observed by Jacobs[13] and by measuring the temperature dependences of a number of the transitions. They were able to associate most of the transitions with specific pairs and to assign ground-state spin quantum numbers as well. Our results are in complete agreement with theirs. This gives us some confidence not only that the energy-level scheme devised by Kisliuk *et al.* is correct, but that the chronospectroscopic technique is useful as a direct method for classifying transitions by pair type.

IX. TEMPERATURE DEPENDENCE OF ENERGY TRANSFER PROCESS

Imbusch[12] noted a decrease in the intensities of the N lines relative to the R_1 line as the temperature is lowered below 50 °K. To account for this decrease he postulated that the transfer process from the higher energy ^2E level, the $2\bar{A}(^2E)$ level, was more efficient than from the lower $\bar{E}(^2E)$ level. Decreasing the temperature with the consequent depopulation of $2\bar{A}$ would thus lead to an over-all decrease in the efficiency of the transfer process.

It is not hard to calculate the effects of this mechanism on the null-point phase of the R_1 line. Figure 10 shows the relevant energy levels and transition probabilities. Transfer to all pairs is symbolized by the single generic pair level. If we define

$$w_1 = w_{1g} + w_{1p} , \tag{12}$$

where w_{1g} and w_{1p} are the probabilities per unit time for transitions from the $\bar{E}(^2E)$ level to ground and to all pairs, respectively, and if we further define

$$w_2 = w_{2g} + w_{2p} \tag{13}$$

for similar transitions from the $2\bar{A}(^2E)$ level, the rate equations become

$$\dot{n}_1 = -w_1 n_1 - w n_1 + w e^{\Delta/kT} n_2 , \tag{14}$$

$$\dot{n}_2 = -w_1 n_1 + w n_1 - w e^{\Delta/kT} n_2 , \tag{15}$$

where w is the probability of a transition from $\bar{E}$ to $2\bar{A}$ and $w^{\Delta/kT}$ is the probability for the reverse transition. We expect w_1 and w_2 to be on the order of the inverse lifetimes of the ^2E levels or about

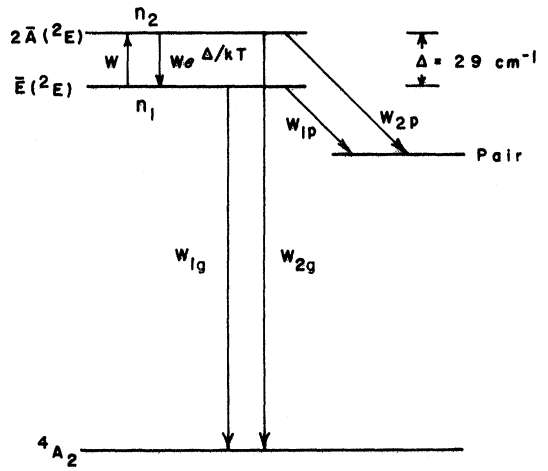

FIG. 10. Energy-level scheme for transitions from ^2E levels to ground-state $^4A_2$ and all pair levels symbolized by the level labeled "pair". Populations of the ^2E levels are given by n_1 and n_2, and transition probabilities per unit time by the w's.

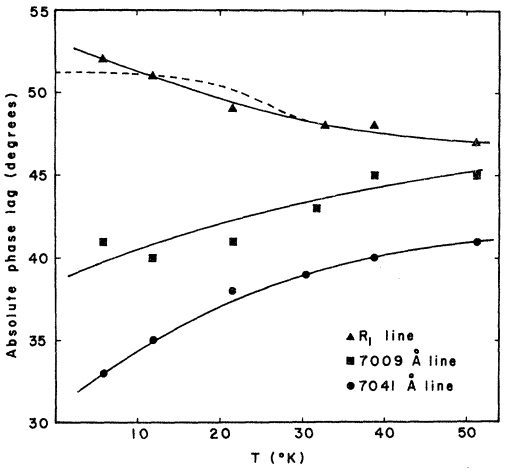

FIG. 11. Temperature dependence of null-point phases of R_1, 7009- and 7041-Å lines taken at 45.6 Hz. Temperatures were measured with a GaAs diode. Phase angle is given relative to the pump light. Dashed line is theoretical curve for $w_1 = 230$ cm^{-1} and $w_2 = 353$ cm^{-1} in Imbusch's model.

250 sec^{-1}. The relaxation time between the $2\bar{A}$ and $\bar{E}$ levels has been shown to be given by[14]

$$T_1 = 3.8 \times 10^{-9} e^{\Delta/kT} , \tag{16}$$

so that w is on the order of 10^8 at these temperatures. The approximation that $w \gg w_1$ and w_2 yields a rather simple form for the lifetime of the $\bar{E}$ level

$$\tau = \frac{1 + e^{-\Delta/kT}}{w_1 + w_2 e^{-\Delta/kT}} . \tag{17}$$

Figure 11 shows the experimentally measured values of the null-point phases of the R_1, 7009- and 7041-Å lines as a function of temperature. The solid lines indicate the best-fit graphs of the points. The dashed line is the theoretical curve of $\phi = \tan^{-1} \omega\tau$ where τ is given by Eq. (17). Values of w_1 and w_2 were taken to be 230 and 353 sec^{-1}, respectively, to fit the points at 10 and 50 °K.

Above 35 °K these values give a very good correspondence of theory with experiment. However, at low temperature, there should be no significant change in τ until $w_2 e^{-\Delta/kT}$ becomes a significant fraction of w_1; for $\Delta = 29$ cm^{-1} this would occur for $T > 15$ °K or so. In fact there was a definite decrease in τ in the range from 5 to 10 °K as is indicated on the graph. Possibly the energy transfer interaction itself is temperature dependent.[15]

X. INTRINSIC PUMPING OF FOURTH NEIGHBORS

In addition to the R lines, the single chromium ion in ruby has a number of other transitions bearing on these experiments. There are broad absorption bands centered at about 18 000 and 25 000 cm^{-1}, termed the U and Y bands, respectively, and a number of sharp-line transitions near 21 000 cm^{-1}, the B lines.

In the past little attention has been given to the possible effects of the presence of a near-neighbor chromium ion on these levels. One would assume that an exchange interaction would shift these levels somewhat, just as happens for the $^4A_2$ and ^2E levels, but not radically alter them. It is thus somewhat surprising that Imbusch saw no intrinsic pumping of ion-pair bands in his energy transfer experiments.

With a few minor changes in our experimental setup we were able to find a number of levels associated with fourth-neighbor pairs. The spectrometer was set to 7009 Å to continually monitor the N_2 line, the strongest pair line in fluorescence. The pump light was then swept downward in wavelength from 6200 to 4200 Å, an interval covering the U band, B lines, and part of the Y band. Since the lifetimes of the excited pair states are very much shorter than those of the single-ion ^2E levels, intrinsic pumping of any fourth-neighbor pair bands ought to be evident in a corresponding decrease in the null-point phase.

Figure 12 shows the apparatus. A $\frac{1}{4}$-m Jarrel-Ash grating monochrometer was used to sweep the pump-light wavelength. The bandwidth of the pump light was about 50 Å, admittedly rather large, but any smaller bandwidth than this would have reduced

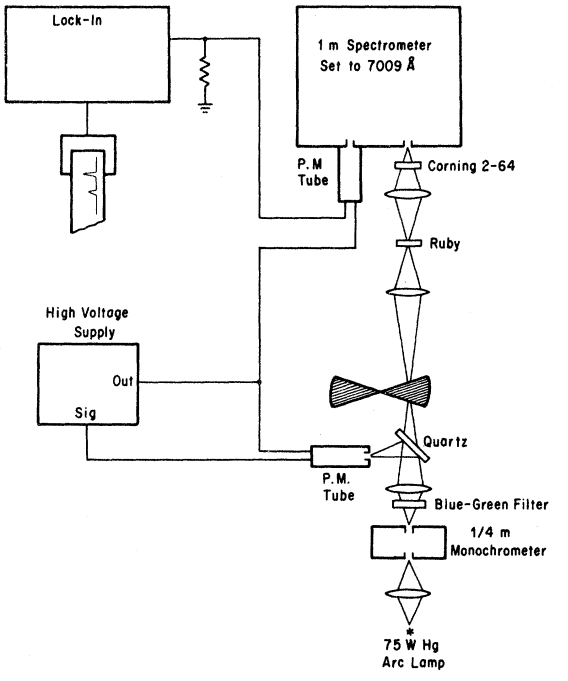

FIG. 12. Apparatus used in selective excitation of 7009-Å line.

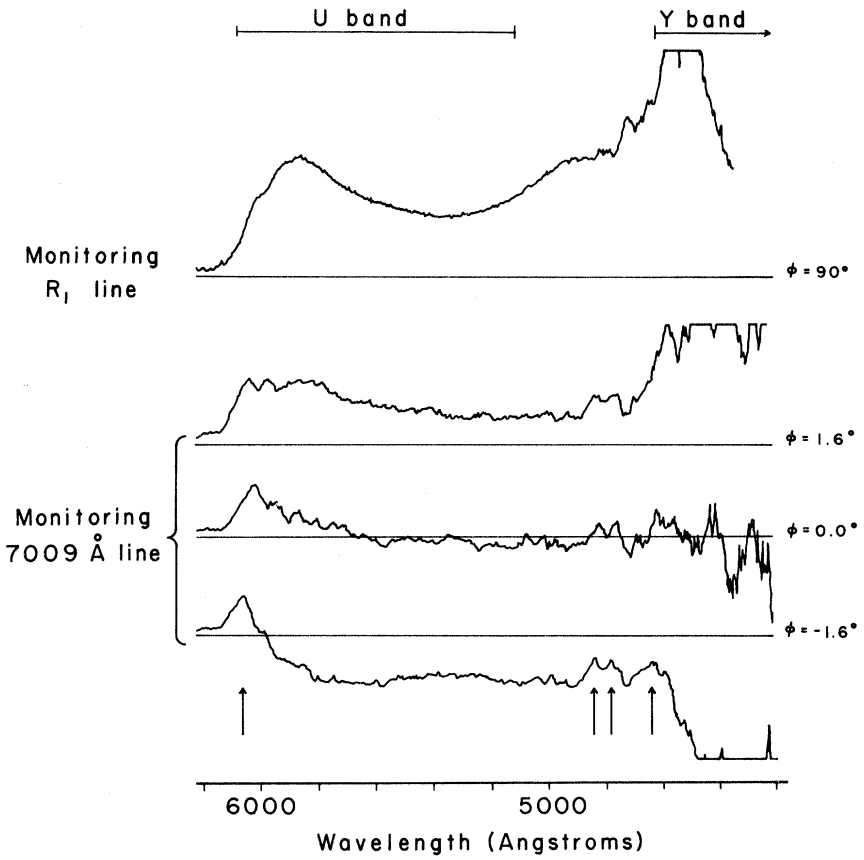

FIG. 13. Results of selective excitation of 7009-Å line at 45.6 Hz and 77.4 °K. Arrows indicate possible excited levels of fourth-neighbor pair. Phase is given relative to an arbitrary zero.

the pump intensity to too low a level.

Several precautions were taken to eliminate spurious effects which might arise. A xenon arc lamp was used as a pump source because, unlike a mercury lamp, the visible spectrum of a xenon arc is relatively smooth over the range of interest. In addition, a second photomultiplier tube, identical to the first, was used to monitor the pump-light intensity. The signal from the pump monitor phototube passed through a negative feedback circuit to control the voltage, and thus the gain of the first tube. This was done to compensate for changes in the pump-light intensity.

The results are shown in Fig. 13. The diagram at the top shows the signal from the R_1 line for comparison. The limits of the U and Y bands are indicated. The bottom three curves show the spectrum for different values of the phase. The arrow near 6050 Å on the bottom diagram indicates a feature with a significantly shorter time constant than the U and Y bands. This feature is most probably an intrinsic band or energy level of the fourth-neighbor pair shifted downward in energy from the single-ion U band by exchange. The three arrows at 4650, 4770, and 4850 Å also indicate features with shorter time constants than the background. These may arise from the Y band from fourth-neighbor exchange interactions.

This experiment was severely limited by a small pump-light intensity and low resolution due to large pump bandwidth. Both of these disadvantages could be overcome with the use of a tunable-dye laser, a device which is unfortunately, unavailable to us in this laboratory. Using this technique and with adequate pump light and resolution, much of the energy-level shceme, possibly even including those levels arising from the single-ion ^2E levels, could in principle be constructed for each pair type.

ACKNOWLEDGMENTS

We would like to thank Carson D. Jeffries for his support for this work. We have also benefited from helpful discussions with James P. Wolfe and Peter L. Scott.

*Supported in part by the U. S. Atomic Energy Commission, Report No. UCB-34P20-154.

[1]S. Sugano and Y. Tanabe, J. Phys. Soc. Japan 13, 880 (1958).

[2]A. L. Schawlow, D. L. Wood, and A. M. Clogston, Phys. Rev. Letters 3, 502 (1959).

[3]A. L. Schawlow, in *Quantum Electronics* (Columbia U. P., New York, 1960).
[4]P. Kisliuk, A. L. Schawlow, and M. D. Sturge, in *Advances in Quantum Electronics* (Columbia U. P., New York, 1964), p. 725.
[5]P. Kisliuk and W. F. Krupke, J. Appl. Phys. 36, 1025 (1965).
[6]P. Kisliuk and W. F. Krupke, Appl. Phys. Letters 3, 215 (1963).
[7]P. Kisliuk, N. C. Chang, P. L. Scott, and M. H. L. Pryce, Phys. Rev. 884, 367 (1969).
[8]A. A. Kaplyanskii and A. K. Przhevuskii, Dokl. Akad. Nauk. SSSR 142, 313 (1962) [Sov. Phys. Doklady 7, 37 (1962)].
[9]L. F. Mollenauer and A. L. Schawlow, Phys. Rev. 168, 309 (1968).
[10]G. F. Imbusch (private communication).
[11]A similar method was used almost twenty years ago by A. Schmillen to measure the fluorescent lifetimes of certain organic substances. See A. Schmillen, Z. Physik 135, 294 (1953).
[12]G. F. Imbusch, Phys. Rev. 153, 326 (1966).
[13]Stephen F. Jacobs, The Johns Hopkins Spectroscopic Report No. 24, 1969 (unpublished).
[14]S. Geschwind, G. E. Devlin, R. L. Cohen, and S. R. Chinn, Phys. Rev. 137, A1087 (1965).
[15]For a further discussion of energy transport mechanisms in ruby, see R. J. Birgenau, J. Chem. Phys. 50, 4282 (1969).

PHYSICAL REVIEW B VOLUME 7, NUMBER 4 15 FEBRUARY 1973

Phonons in Solid Hydrogen and Deuterium Studied by Inelastic Coherent Neutron Scattering

M. Nielsen
Atomic Energy Commission, Research Establishment Risö, DK-4000 Roskilde, Denmark
(Received 14 January 1972; revised manuscript received 18 September 1972)

Phonon dispersion relations have been measured by coherent neutron scattering in solid para-hydrogen and ortho-deuterium. The phonon energies are found to be nearly equal in the two solids, the highest energy in each case lying close to 10 meV. The pressure and temperature dependence of the phonon energies have been measured in ortho-deuterium and the lattice change determined by neutron diffraction. When a pressure of 275 bar is applied, the phonon energies are increased by about 10%, and heating the crystal to near the melting point decreases them by about 7%. The densities of states, the specific heats, and the Debye temperatures have been deduced and found to be in agreement with the published experimental results. The Debye temperatures are 118 K for hydrogen and 114 K for deuterium. For hydrogen the Debye-Waller factor has been measured by incoherent neutron scattering and it corresponds to a mean-square displacement of the hydrogen molecules of 0.48 Å^2.

I. INTRODUCTION

Solid H_2 and D_2 belong to the class of quantum solids (He, H_2, D_2) for which the kinetic energy of the zero-point motion of the particles is comparable with the potential energy, and the amplitudes of vibrations at 0 K are not small compared with the separation of neighboring particles.

The standard methods of lattice dynamics are not applicable to quantum solids, but new methods have been developed and theoretical predictions of the dynamical properties have been published.[1] Most of the theoretical and experimental work in this field has been concentrated on solid He.[2] However, solid H_2 and D_2 are suitable substances for studying the quantum effects because they have a large difference in isotopic mass while their intermolecular potentials are nearly identical, and in addition, they are good materials for neutron scattering experiments.

The forces between the particles in the quantum solids are of the van der Waals type and the pair potentials, which are of the Lennard-Jones form, have parameters which are fairly well known from the properties of the gas phases. Owing to the large zero-point motion and the hard-core repulsion in the pair potential at small separations, the crystals are expanded and the distance between the neighboring particles is considerably larger than the distance corresponding to the minimum in the pair potential. Furthermore, short-range correlations in the motion of the particles must be introduced to prevent overlap of the single-particle wave functions in the hard-core region of the pair potential.

To account for the short-range correlations in the ground-state wave function Nosanow[3] introduced a Jastrow factor

$$f(R) = e^{-Cv(R)/2} , \tag{1}$$

where $v(R)$ is the gas-phase pair potential and C is a variational parameter. In calculating the dynamical properties, the short-range correlations are taken into account by replacing $v(R)$ by an effective potential,

$$W(R) = f^2(R)\left(v(R) - \frac{\hbar^2}{2M}\nabla^2 \ln f(R)\right) . \tag{2}$$